Adsorption and superficial transport of oil on biological and bionic superhydrophobic surfaces: a novel technique for oil–water separation

W. Barthlott[1], M. Moosmann[1], I. Noll[2], M. Akdere[2], J. Wagner[2], N. Roling[1], L. Koepchen-Thomä[1], M. A. K. Azad[1,†], K. Klopp[3], T. Gries[2] and M. Mail[1,‡]

[1]Nees Institute for Biodiversity of Plants, University of Bonn, Venusbergweg 22, 53115 Bonn, Germany
[2]Institut für Textiltechnik, RWTH Aachen University, Otto-Blumenthal-Strasse 1, 52074 Aachen, Germany
[3]Heimbach GmbH, An Gut Nazareth 73, 52353 Dueren, Germany

Subject Areas:
chemical physics, environmental chemistry, materials science, physical chemistry, environmental engineering, fluid mechanics

Keywords:
oil adsorption, oil spill clean-up, air retention, *Salvinia* effect, textile, biomimetics

Author for correspondence:
W. Barthlott
e-mail: barthlott@uni-bonn.de

†Present address: School of Sciences, Brac University, 41 Mohakhali, Dhaka 1212, Bangladesh.

‡Present address: Karlsruhe Nano Micro Facility, Karlsruhe Institute of Technology, Hermann-von-Helmholtz-Platz 1, 76344 Eggenstein-Leopoldshafen, Germany.

Superhydrophobicity is a physical feature of surfaces occurring in many organisms and has been applied (e.g. lotus effect) in bionic technical applications. Some aquatic species are able to maintain persistent air layers under water (*Salvinia* effect) and thus become increasingly interesting for drag reduction and other 'bioinspired' applications. However, another feature of superhydrophobic surfaces, i.e. the adsorption (not absorption) and subsequent superficial transportation and desorption capability for oil, has been neglected. Intense research is currently being carried out on oil-absorbing bulk materials like sponges, focusing on oleophilic surfaces and meshes to build membranes for oil–water separation. This requires an active pumping of oil–water mixtures onto or through the surface. Here, we present a novel passive, self-driven technology to remove oil from water surfaces. The oil is adsorbed onto a superhydrophobic material (e.g. textiles) and transported on its surface. Vertical and horizontal transportation is possible above or below the oil-contaminated water surface. The transfer in a bioinspired novel bionic oil adsorber is described. The oil is transported into a container and thus removed from the surface. Prototypes

have proven to be an efficient and environmentally friendly technology to clean oil spills from water without chemicals or external energy supply.

This article is part of the theme issue 'Bioinspired materials and surfaces for green science and technology (part 3)'.

1. Introduction

Oil and its derivatives play a role in several areas of daily life and are still one of the most important energy sources. However, they are, and continue to be, a major global environmental pollutant [1], and bionic (biomimetic) technologies may provide, like in many other fields (survey in [2]), a technical 'bioinpired' solution.

The '*Deep Water Horizon*' in 2010 was the most recent obvious case, when about 780 million litres of crude oil were released into the sea [3].

However, a much greater and common risk are found to be small, seemingly trivial accidents [4]. One study estimates that oil spills amounting to 30 million litres a year in the USA [5] are usually caused by minor events, such as car accidents, boating accidents, floods, and incidents in docks, e.g. in routine work such as loading and unloading of ships, etc. [6]. Oil films on the water surface specifically disturb gas exchange through the water surface and therefor endanger many biological life forms bound to water surfaces (e.g. water striders, birds, etc.) [7]. Surface oil films present a long-term risk for the entire ecosystem and can spread quickly in a large area over connected waterways [7–10].

The removal of oil films is a technical challenge. A growing community is investigating options for the clean-up of oil spills [11], usually with the focus on marine disasters [12]. Thus, most of the existing methods have been designed primarily for offshore use [12]. Above all, oil barriers (prevention of oil spreading on the water surface), skimmers (collection of the oil surface in a vessel just below the surface), sorbents (absorption of the oil and removal from the water surface or sinking of the oil-containing absorber), dispersing agents (dissolution of oil in the water to reduce the concentration) and the burning of the oil are notable [4,13,14].

The separation of water and oil is difficult. Most methods are based on the principle of filtration and thus require an active pumping of the oil–water mixture through the filter material [11,15–17].

A rather overlooked principle that does not require active pumping of the liquids to be separated is the adsorption of the oil onto a surface, subsequent transportation of the oil along this surface and desorption into a collecting vessel.

Several biological surfaces show superhydrophobic properties (surveys in [18–20]). Until now, these surfaces were mostly analysed concerning their self-cleaning capabilities (lotus effect) [21] and their ability to maintain stable air layers under water (*Salvinia* effect) [22–24]. The air retention capability has been analysed mainly for the development of drag-reducing ship hull coatings, anti-fouling coatings [25] and sensory devices [26]. Some of these surfaces show superhydrophobic and oleophilic properties [27–30]. It was observed that some of these surfaces are able to adsorb, transport (figure 1; electronic supplementary material, video V1) and desorb oil.

A promising class of materials for the development of adsorbing and transporting surfaces are textiles, because of their inherent flexible nature and multiscale structure. Textiles can be constructed to incorporate various properties regarding filament, fabric and surface coating.

To understand the underlying principles, biological and technical surfaces, yarns and textiles were investigated with regard to their oil adsorption, desorption and transportation properties. The transport quantities of such surfaces and the maximum achievable transport height are determined. The results are the basis for the development of bionic functional textiles for oil removal, which represent a sustainable, cost-effective and passive alternative to previously used oil separation technologies. These textiles allow the development of a passive, buoyant device that can be used for water purification and contamination containment.

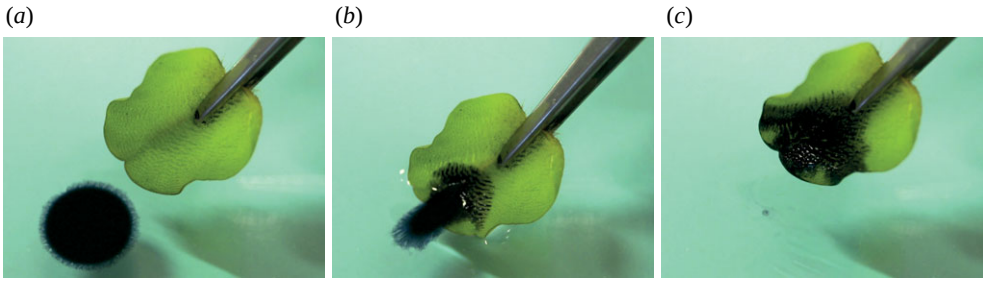

Figure 1. (*a–c*) A crude oil droplet on a water surface is adsorbed by a leaf of *S. molesta* within seconds and transported on the *Salvinia* surface above the water level. See also electronic supplementary material, video SV1. (Online version in colour.)

2. Material and methods

(a) Biological surfaces

Over the last decades, about 20 000 species have been analysed by scanning electron microscopy (SEM) for surface structures and properties by members of our working group (survey and references in [19]). For this study, due to their excellent performance, we selected five plant species (accession numbers of the Botanical Gardens Bonn in brackets) out of 200 different species, all taken from the living collection of the Botanical Gardens of the University of Bonn and tested for their oil adsorption properties: young, but fully developed, upper (adaxial) sides of the leaves of *Cistus albidus* (Cistaceae) (BGB 214536-15); *Pistia stratiotes* (Araceae) (BG BONN 1077); floating leaves of the floating fern *Salvinia molesta* (Salviniaceae) (BG BONN 14459); immature, still green, fruit (siliguae) surfaces of *Fibigia triquetra* (Brassicaeae) (BG BONN 06870); and the lower (abaxial) leaf side of young, but fully developed, leaves of *Helianthemum apenninum* (Cistaceae) (BG BONN 32438) have all been investigated.

(b) Technical surfaces

Five different technical surfaces are investigated for their oil-adsorbing and -transporting properties. The surfaces are hydrophobized by spray coating with Tegotop 210 (Evonik) using an air-brush system (Revell AIR-100). After 24 h of drying, they are not only superhydrophobic but also oleophilic, allowing an investigation of the influence of the surface structures on the oil adsorption and transportation.

The following surfaces have been chosen for the experiments, as they showed good oil-adsorbing and/or -transporting properties plus a wide range in the size and spacing of their structures: abrasive paper P180 for metal processing (grain material, corundum; average grain size, 82 µm; D-paper, 135–160 g m^{-2}; manufacturer, Lux-Tools, Wermelskirchen, Germany); abrasive paper P400 for metal processing (grain material, corundum; average grain size, 82 µm; D-paper, 135–160 g m^{-2}; manufacturer, Lux-Tools, Wermelskirchen, Germany); flock (material, viscose; length, 0.5 mm; glue, copolyester hot melt adhesive; foil, polyethylene terephthalate (PET); manufacturer, Poli Tape Group, Remagen, Germany); commercial textile oil absorbent 'Cobranol' (manufacturer, Nordison e.K., Bönstrup, Germany); and fibreglass textile (carpet, crop; pol-material, glass fibres; carrier material, glass fibres; yarn spacing, 2.54 mm; manufacturer, TFI-Institut für Bodensysteme an der RWTH Aachen e.V., Aachen, Germany).

(c) Oils used

Four types of oil with differing viscosities are selected, representing relevant oils used in technical applications and therefore often spilled in accidents causing pollution. They are mineral oil (15W40, Ravensberger Schmierstoffvertrieb GmbH, Werther; viscosity at room temperature,

186.7 cP; motors of cars); waste oil (oil mixture from different cars; provider, Bonner Kfz. Werkstatt; viscosity at room temperature, 66.1 cP); bilge oil (oil phase of bilge water, which is an oil–water mixture in the shipping industry; provider, Bilgenentölungsgesellschaft mbH Duisburg; viscosity at room temperature, 147.3 cP); and heating oil (conventional, low-sulfur heating oil; Dossinger GmbH, Oberhausen-Rheinhausen; viscosity at room temperature, 5.6 cP).

The viscosity of the oils is measured at room temperature using a rotation viscometer (Brookfield Digital-Viskosimeter; Model DV-II + Pro).

(d) Structure and wettability, video documentation

Samples are analysed by SEM (Leo 1530, Zeiss Microscopy AG, and Auriga 60, Zeiss Microscopy AG) and digital video microscopy (VHX1000, Keyence Deutschland AG). The oil and water wettability of the surfaces is determined by a contact angle measurement device (OCA20, Data Physics, Germany). The contact angles exceeded 140°; however, because of the extremely structured 'hairy' surfaces (apart from sandpaper), a precise reproducible result was not measurable.

(e) Transport and adsorption on yarns and textiles

Additional to the experiments performed with the five samples described in §2b, different yarns and textiles are tested concerning their water and oil adsorption. In these experiments, the water uptake is taken into account, as, for a practical use of an oil-adsorbing textile, the oil uptake has to be significantly higher than the water uptake. Tests are conducted by capturing images from charge-coupled device (CCD) cameras each hour for 24 h. The volume reduction in the water or oil basin is measured in millilitres and is used to quantify the adsorption of oil or water in the investigated yarns and textiles. The gear oil/transmission lubricant used did not show any evaporation. In order to account for evaporation of certain fluids at room temperature (e.g. water), the reduction in volume due to evaporation is measured over 24 h in an additional basin. This volume loss is used to correct the directly measured volume loss when evaluating the textile adsorption. Transmission lubricant adsorption and water adsorption are measured as single-phase liquids and not as a mixture.

To determine the influence of viscosity change, water is mixed with 2 and 3 vol% xanthan. For these tests, a mixture of water and xanthan is used instead of oils with different viscosities, as with oils, properties other than only the viscosity might influence the adsorption properties. The increase in viscosity is detected by means of the stick-droplet test and visual inspection

The investigated specimens are:

— textile non-woven: PET (full form),
— textile compound non-woven: three layers of polyethylene (PE), cellulose, polypropylene (PP),
— textile compound non-woven: three layers of PE, cellulose, PP and threefold weight per metre square compared to the previous specimen,
— textile non-woven: one layer of PET,
— textile compound non-woven: three layers of PE, cellulose, PE,
— textile non-woven: artificial mineral fibre,
— textile twist: cotton (Co) fibres,
— textile twist: Co and Aramid fibres,
— textile knit: artificial mineral fibre,
— textile weave: artificial mineral fibre,
— the mass per metre square of the textiles was between 100 and 700 g m^{-2},
— the fibre diameter was between 50 and 250 µm.

(f) Adsorption capacity measurement

To determine the oil adsorption capacity of the biological and technical surfaces and the dependence on the viscosity of the different oils, samples with a size of 2 cm^2 are investigated. They are weighed and placed flat on the surface of the respective oil, with the oil-adsorbing side facing downward. After 15 s, the samples are removed using tweezers, and are held vertically for 30 s. It is observed that no oil dripped off the samples. The oil-saturated samples are again weighed in order to determine the amount of adsorbed oil. The calculated values are given in relation to the sample size ($g\,m^{-2}$) or in relation to the own weight of the sample (%).

The measurement is done using five samples of each material and with each of the four oils.

In the case of *Fibigia* and *Pistia*, the values measured are divided by a factor of 2, since these samples have an oil-adsorbing structure on both sides of the sample.

(g) Measurement of maximum vertical transportation height and velocity

To determine the oil transport velocity, samples are mounted vertically above an oil-filled container and a camera (Canon EOS 650D, software Eos Digital 5.0) is directed towards the sample surface. The container is lifted until the oil is in contact with the end of the oil-adsorbing sample. Subsequently, the oil is adsorbed and transported at the surface against gravity. The process is recorded and images are taken at defined time intervals.

Based on these recordings, the transport height reached at the specific times is determined and these values are used to determine the rate of oil transport.

The measurements are carried out on five samples each of the same material and with each of the four oils. For each sample, the transportation height is measured at three points to exclude material-related irregularities.

(h) Analysis of the thickness profile of the oil film

To analyse the thickness profile of the oil layer adsorbed, oil-containing biological and artificial samples are frozen using liquid nitrogen. Subsequently, the frozen samples are broken and their cross-sections are analysed using a digital light microscope. This allowed the measurement of the film thickness and analysis of its cross-section.

(i) Simulation of the oil transport on hydrophobic surfaces

All five species analysed have trichomes (hairs) on their leaf surface. Considering a section parallel above the leaf surface, the trichomes can be approximated as circles in a surface. The oil is transported between these circles.

The distances between these circles (trichomes) are in the sub-millimetre range. In this scale, mainly surface and capillary forces are dominant [31]. Bashir *et al*. [32] showed that problems in the microfluidic range can be solved numerically. Chen *et al*. [33] showed that such a problem can be simulated using a volume of fluid (VoF) model. In order to investigate the influence of different parameters, such as hair diameter or distance of the oil transport, the process is simulated using ANSYS Fluent (VoF) [34].

In order to investigate the influences of these parameters on the transport behaviour, it is sufficient to consider a small cell of a typical cross-section of the biological models. A base area of 1.3 mm × 0.9 mm contains six (partial) circles of 0.6 mm diameter similar to the trichomes of *S. molesta* (see §3d).

These circles are assigned a contact angle of 20°, which is determined through initial experiments on the biological role models. The fluid flow area in between the hairs is modelled by a mesh of 2500 elements. On the left side, there is a pressure-free inlet for the oil (ANSYS Database), while on the right side, air can escape as the boundary conditions are set to atmospheric conditions. The surface tension between the two phases is 34 $mN\,m^{-1}$ [35].

A transient method is used to capture the changes in the fluid domain. The inlet velocity is used as a comparison variable for evaluation. The influence of the mesh size is investigated using different mesh scales from 1000 elements up to 4000 elements for the area. The flow remains laminar due to the low speed and the Reynolds number is much smaller than 10.

3. Results and discussion

(a) Biological surfaces

Adsorption and transport velocities for four different types of oil on the five plant surfaces are shown in figure 2. Oils with a high viscosity are transported much faster in almost all cases than oils with a low viscosity. Transport velocity and the maximum oil transportation height strongly depend on the architecture of the adsorbing surface. All surfaces investigated are hydrophobic or superhydrophobic and oleophilic. The best transportation properties are observed in dense hairy surfaces. The dependence of the transportation velocity on the hair density is predominantly observed and can be demonstrated in *Salvinia* and *Fibigia*. In both species, the hair density changes towards the marginal areas of *Salvinia* and the central area in *Fibigia*. Here, the trichomes are significantly denser (average hair distance of *Salvinia* $244.29 \pm 38.27\,\mu m$ and *Fibigia* $235.47 \pm 28.12\,\mu m$), and thus the transportation speed increases. *Cistus* shows the lowest indumentum density, but additionally a strong structuring given by the prominent leaf veins, which also enhances transport. Accordingly, with regard to a bionic surface, an alternative to a hairy surface may be a surface with many small ridges. The most important prerequisite for a particularly high capillary interaction between the hairs is their separation distance and not their length. This can be observed with *Salvinia* [36]. The leaves are divided into areas with different hair densities and hair lengths. The apical leaf part, with its small trichomes which are close together, transports oil much faster than the central area. Additionally, the number of contact points between the hairs seems to be important for oil transport. A small hair distance is usually associated with greater contact between the trichomes. In *Salvinia*, the ends of the eggbeater-shaped trichomes [36] touch each other in the apical portion, transporting more oil in the marginal than in the central area. The oil film thickness on the leaves is significantly less than the length of the trichomes. Thus, the resulting capillary effect is dependent more on the distance between the hairs than on the length.

(i) Adsorption capacity measurement

It was concluded that *Salvinia* and *Cistus* have the highest and lowest adsorption capacity, respectively. The adsorption capacity also depends on the viscosity of the oil. Due to its high viscosity, the highest adsorption capacities of all surfaces in the experiments are reached with mineral oil 15W40. This dependence of the adsorption capacity on the viscosity of the oil could be seen on the surface of *Cistus*, where capacity increases with increasing viscosity. *Cistus* shows the lowest density of hairs. Low-viscosity oil, due to the vertical measuring method, can quickly flow down the leaf surface, since it is only held up to a small extent by the hairs.

(ii) Measurement of maximum vertical transportation height and velocity

With increasing oil viscosity, the transport speed on the surfaces decreases. *Pistia* and *Fibigia* obtained the highest performance based on the results of the experiments. *Fibigia* and *Salvinia* show different transport properties at different points of the surface (edge/middle). *Fibigia* performs best in the central surface area of the fruit, and *Salvinia* in the margin of the leaf surface. The transportation properties of *Salvinia* in the central area of the leaf show almost no change after cutting the tips of the eggbeater-like shaped trichomes. This is in accordance with the results of the freezing tests (figure 3), in which no oil in this leaf area came into contact with the eggbeater-shaped apical portion of the trichomes.

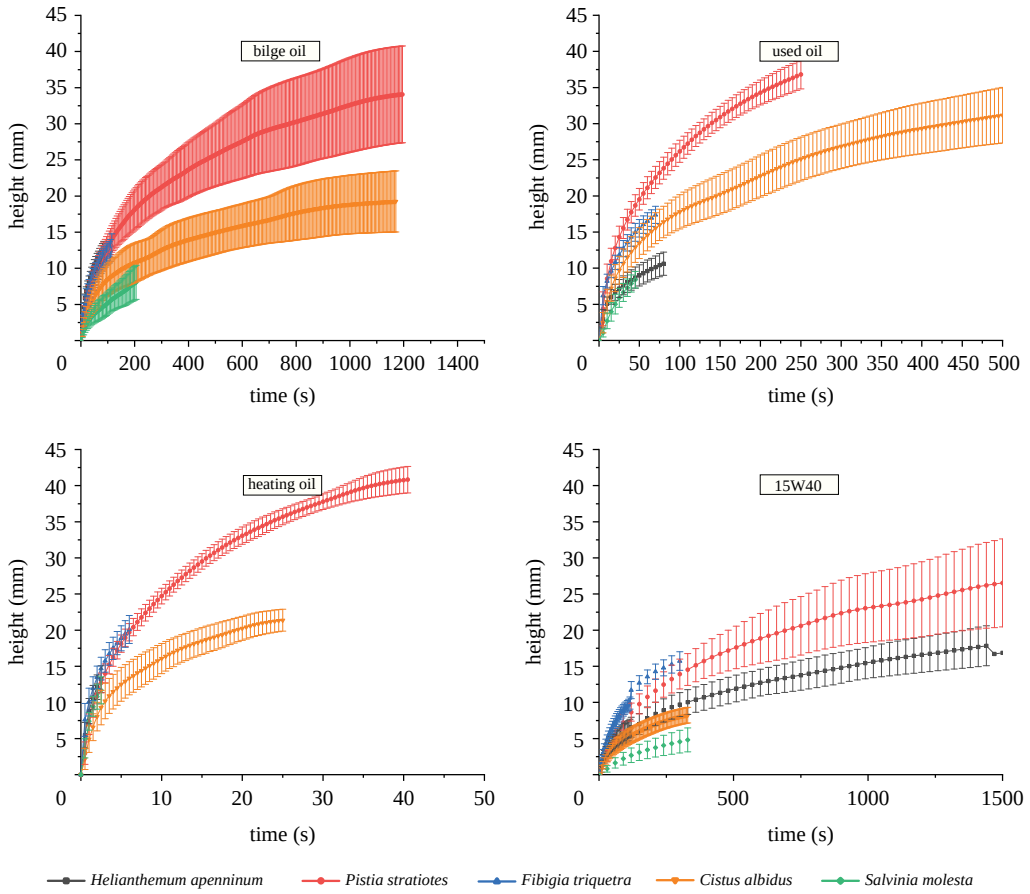

Figure 2. Transportation height over time on the investigated plant surfaces. In each diagram, the results for one of the four oil types are shown. (Online version in colour.)

(iii) Analysis of the thickness profile of the oil film

The investigation of the frozen and broken samples shows that the surface structures in most cases are not filled to the tips with oil (figure 3). The film thickness also significantly depends on the viscosity of the oil.

When an air-retaining surface is submerged under water and one end is in contact with an oil film at the water surface, oil is adsorbed by the surface and transported under water (figure 4; electronic supplementary material, videos SV2 and SV3). Air is thereafter replaced by oil (figure 4). This might open new possibilities for bionic applications.

(b) Technical surfaces

The results of technical surfaces are similar to those with plant surfaces.

They show a significant dependence of the transport properties and the absorption capacities on the viscosity of the respective oil as well as a dependence of these properties on the surface structure.

(i) Adsorption capacity measurement

Regarding the oil absorption capacity, especially the commercial textile oil absorbent (Cobranol) showed a high capacity of up to 8.5 times its own weight. The oil is absorbed on the surface and

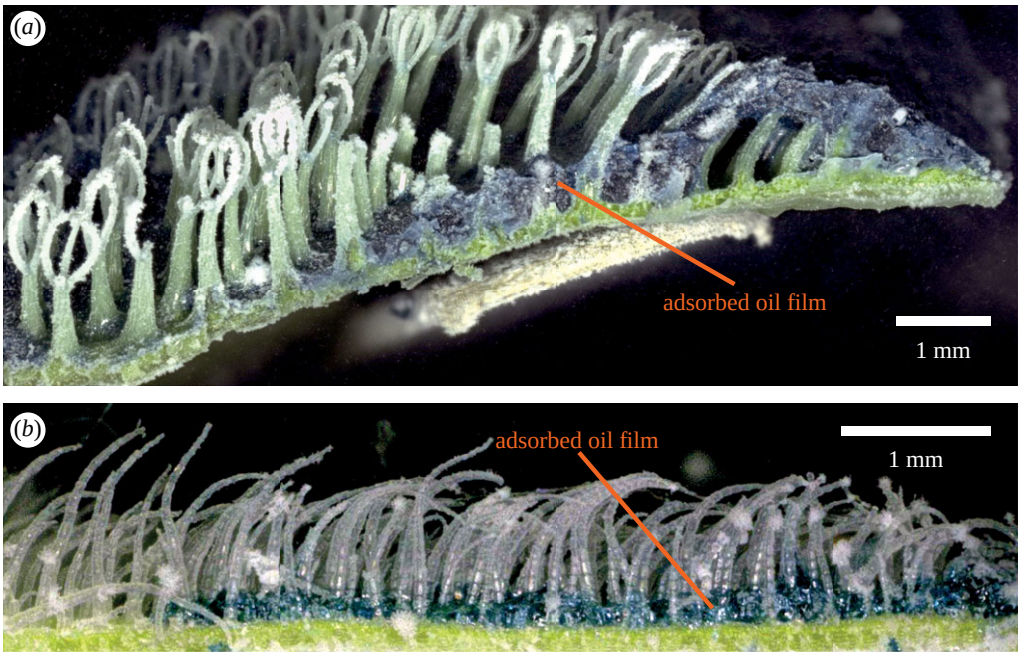

Figure 3. Cryo section of a leaf of (*a*) *S. molesta* and (*b*) *P. stratiotes* covered by an adsorbed oil film. The shock frozen samples analysed in a digital microscope reveal the position of the oil film on the surface at the base of the complex hairs. (Online version in colour.)

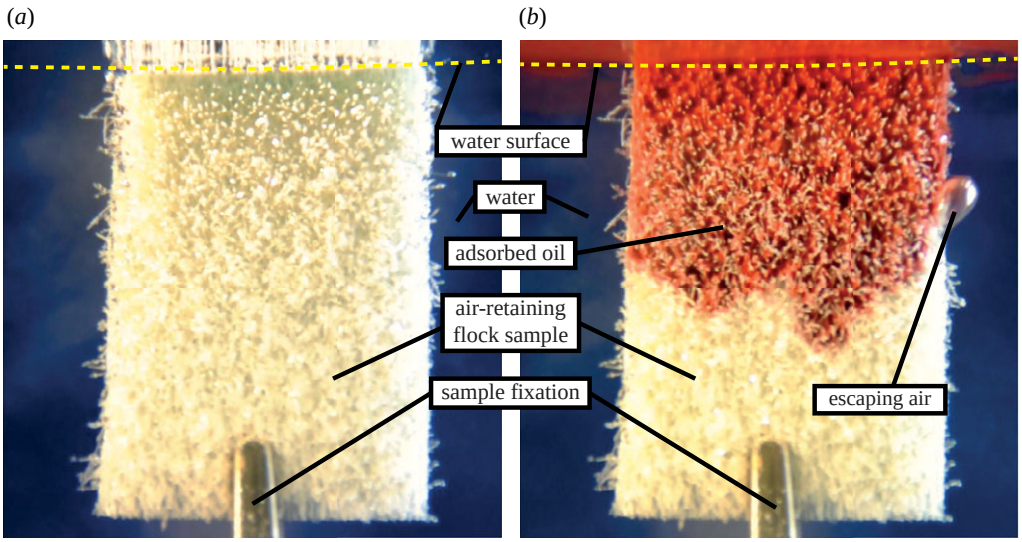

Figure 4. (*a*) Hydrophobic flock surface immersed in water and (*b*) after contact with an oil film (stained red) on the water surface (dotted yellow line). The oil is quickly adsorbed and transported under and against gravity above the water surface. The air layer within the dense indumentum is replaced by an oil layer. See also electronic supplementary material, videos SV2 and SV3. (Online version in colour.)

in the material, meaning absorption is a physical principle. Concerning the adsorption of oil on the surface, the glass fibre textile showed a very high capacity of up to 2.85 times its own weight. This textile has very long and dense fibres, which cause large capillary forces and thus adsorb a high quantity of oil.

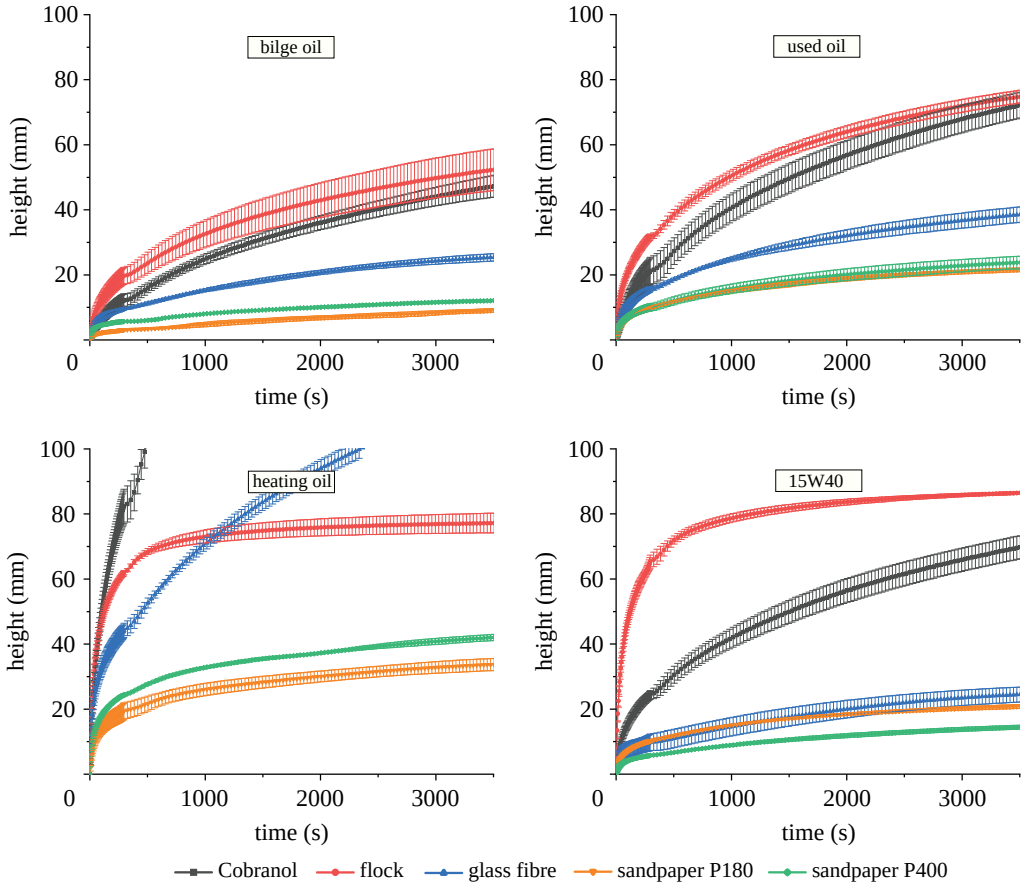

Figure 5. Transportation height over time on technical surfaces. In each diagram, the results of one of the four oil types are shown. (Online version in colour.)

(ii) Measurement of maximum vertical transportation height and velocity

Technical materials transport oils with a low viscosity better than oils with a high viscosity (figure 5). The absorbing (not adsorbing) textile oil absorbent (Cobranol) has the highest performance characteristics. It is able to transport heating oil within 44 min 180 mm above the water–oil film level. This means an average velocity of 0.07 mm s^{-1}, but, as could be seen in figure 5, in all cases, the velocity strongly depends on the height already reached. The lowest transportation is measured in the two sandpaper surfaces, which, depending on the oil, reached a maximum height of 30 mm in the same time. The flock surface performed best of the adsorption-based materials. When mineral oil 15W40 is used, a transport height of 85 mm could be achieved within 30 min. However, also here a strong dependence on the viscosity of the oils is seen (figure 5). In addition to the vertical transport speed and the maximum height absorption investigations, the maintenance of transport properties for horizontally arranged materials is tested. In this preliminary experiment, after eight weeks, no change in the transport properties could be determined. This is a very promising result concerning the permanent use of a bionic oil adsorbent textile.

(c) Transport and adsorption on yarns and textiles

As a first understanding of the results shown in figure 6 and the visual inspected adsorption videos of the CCD testing device, the different specimens adsorb the fluids in 6–24 h. Selected

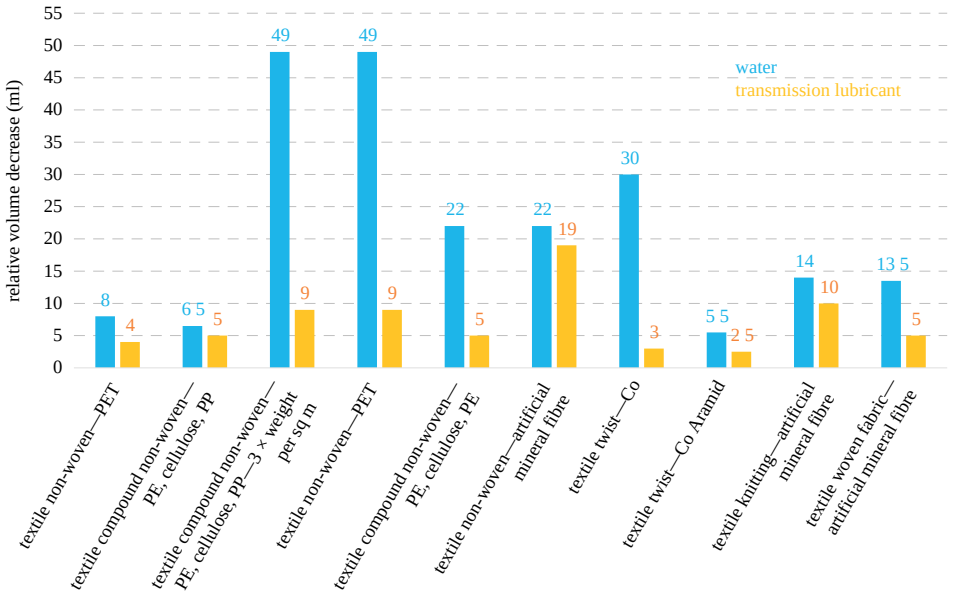

Figure 6. Transmission lubricant and water adsorption in different yarns and textiles described in §2e after 24 h. (Online version in colour.)

specimens have a higher water adsorption than transmission lubricant adsorption. The maximum water adsorption in 24 h was 49 ml of the non-woven textile made of three layers PE, cellulosic fibres and PP and a non-woven textile made of PET. Even a technical yarn twist made of cotton reached a level in water adsorption of 30 ml after 24 h. The specimen with fibres of cellulose (artificial cellulose and cotton) achieved the highest water adsorption levels. An increase in water adsorption could be achieved by means of the increase in mass (g mm^{-2}) of the textiles. Most materials are more likely to adsorb water than oil. Only the non-woven textile made of artificial mineral fibres showed similar adsorptions for transmission lubricant and water. Based on the fact that high amounts of water could be wrung out of the specimen after the experiment, adsorption must have been the predominant mechanism. The results performed with water and water mixed with 2 and 3 vol% xanthan are shown in figure 7. The increase in viscosity of water leads to a reduction in water adsorption of the investigated non-woven textile specimen. The water and transmission lubricant adsorption of yarn textiles depend on fibre diameter, mass and fluid viscosity. The adsorption of 49 ml water required 6–24 h depending on the textile and its material. It is concluded that these textiles have a low adsorption velocity. For industrial applications, higher velocities are required.

Textiles are particularly suitable for the technical transfer of complex biological surface structures for the production of bionic adsorber materials, since the hierarchic structure could mirror that seen in nature. Another advantage is the high adjustability of the properties through the material selection of, for example, hydrophilic or hydrophobic polymers and their characteristics in fineness, cross-sectional geometry or textile structures such as fleece, woven, knitted, braided or tufted structure (carpet).

(d) Simulation of oil transport on hydrophobic surfaces

The velocity distributions and the motion of the individual fluid elementary particles can be displayed and evaluated in different views. This allows a detailed inside view into the interaction of the oil with the individual filaments in the textile and with the hairs in the biological model, with which the effects of the influencing parameters can be investigated. Crucial parameters for

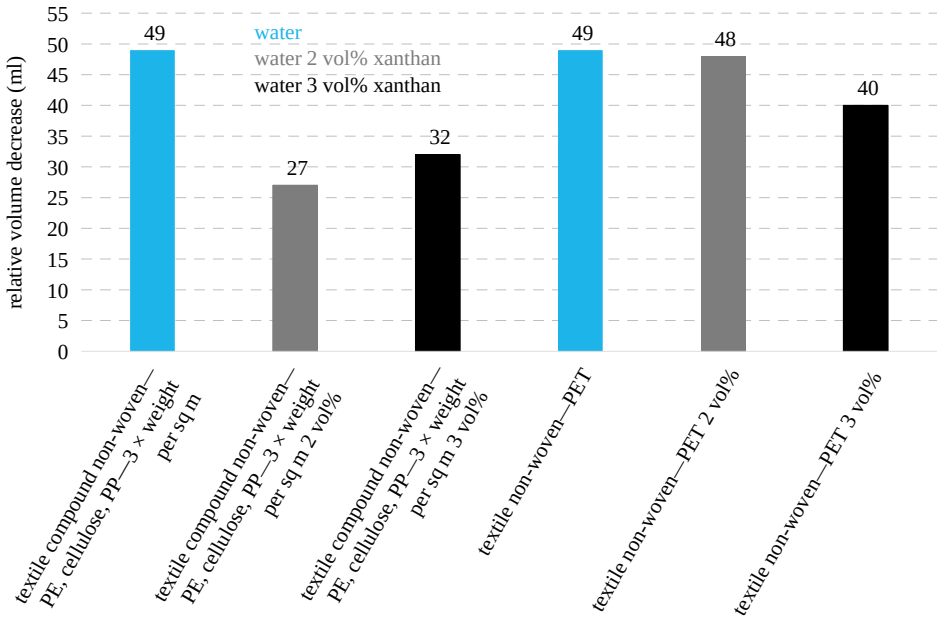

Figure 7. Change in adsorption by means of viscosity increase in water after 24 h measured on samples described in §2e. (Online version in colour.)

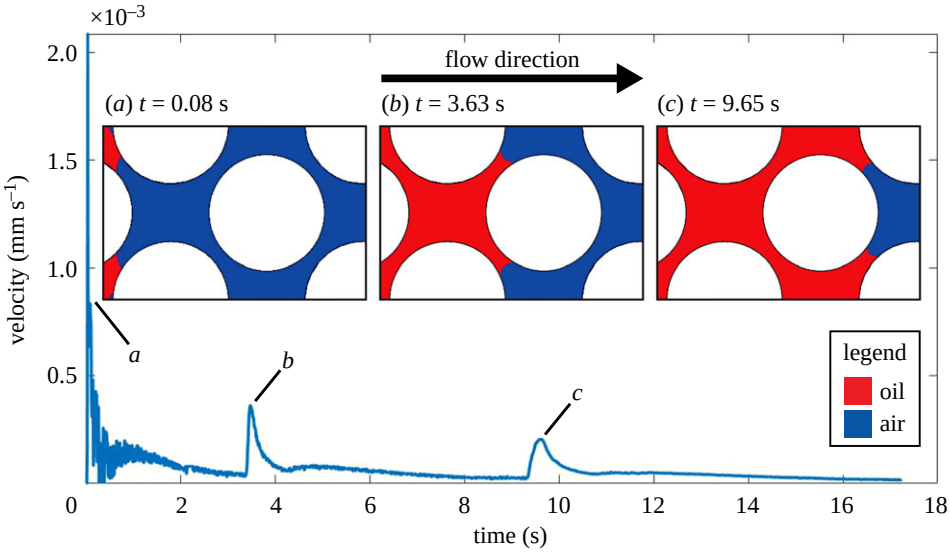

Figure 8. Oil flow velocity during transport through the model. Crucial are the bottlenecks (*a*–*c*) between the hairs where the speed reaches a local maximum. (Online version in colour.)

the simulation are the contact angle, the surface tension and the distance between the hairs. In order to assess the transport velocity of different geometric arrangements and oils, a velocity graph showing the mean velocity at the inlet over time is generated. This shows that the initial velocity decreases continuously after an impulsive rise, whereas there is a dependence on the geometric arrangement. When a filament row meets the adjacent one, capillary junctions (figure 8*a*–*c*) are present, which cause a local acceleration of the oil transport. Huang *et al.* [37] also describe, in their studies on the flow of blood in capillaries, a similar drop in velocity after

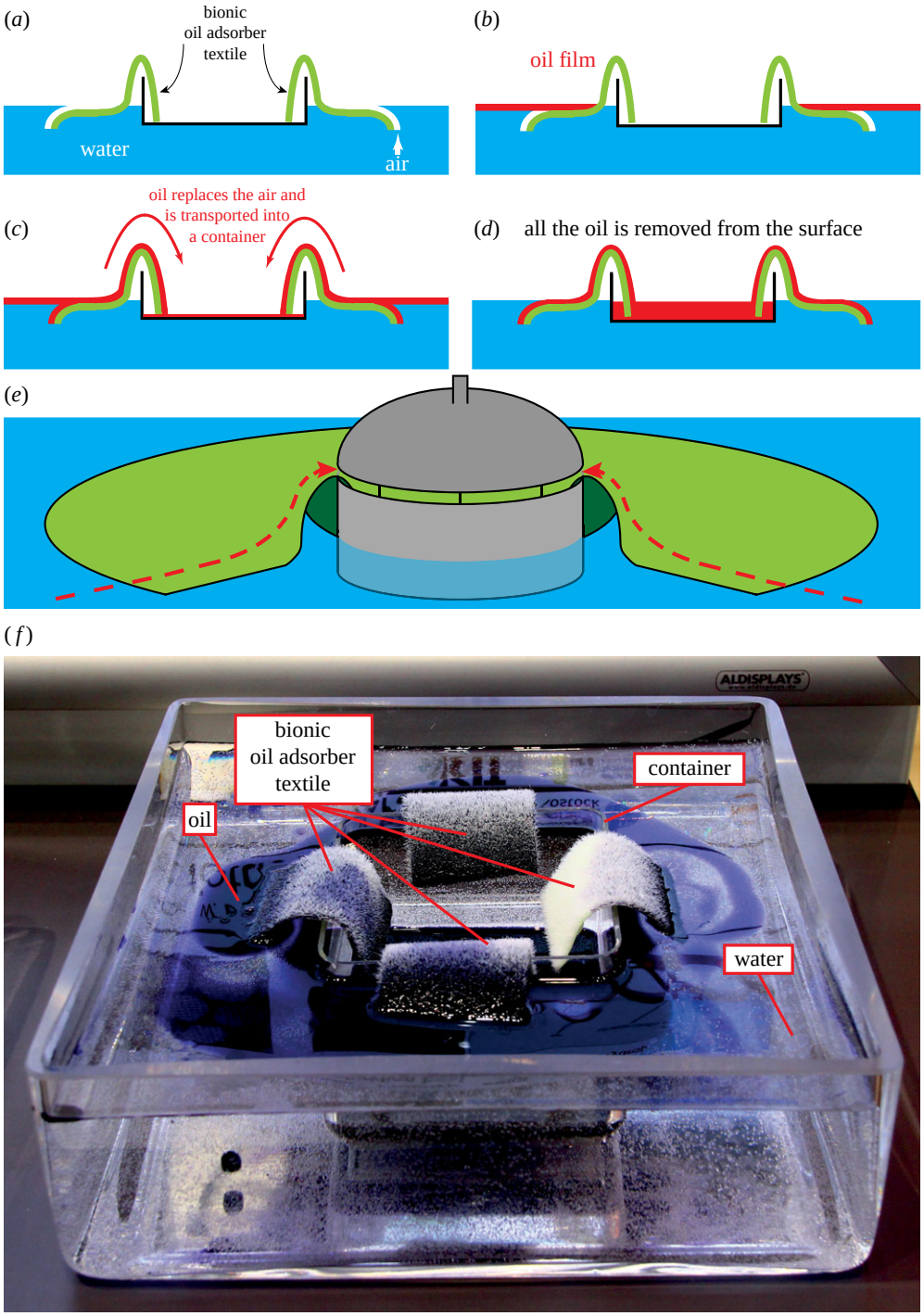

Figure 9. BOA for trapping and removing oil spill from water surfaces. (*a*) Device on a clean water surface. (*b*) The oil film reaches the adsorbing textile. (*c*) Oil is adsorbed and transported on the adsorbing textile surface above the container margin and desorbed into the vessel. (*d*) Spilled oil is trapped in the container (covered by a lid (*e*)), which now can be removed. Detailed explanations in the text. (*f*) Prototype of a floating oil collector. Four superhydrophobic flock strips were mounted onto a plastic container. Oil on the water surface is adsorbed by the flock samples and wets the flock strips. The oil is transported along the surface and collected in the plastic container until the entire oil on the water surface is adsorbed. Colours used in the schematic: blue, water; red, oil; green, adsorbing textile; grey, collecting vessel for the oil captured, covered by a lid when exposed on, for example, a lake. (Online version in colour.)

an initial impulsive beginning. The general decrease in the speed with increasing length of the transport route can also be observed in the biological models.

Based on the matching results of the simulation with the observations of the biological models and those of Huang *et al*. [37], the simulation model can be used to determine the optimal parameters for the textile. By simply varying the parameters (such as diameter or distance of the trichomes) in the model, a preselection of the optimal parameters can be made and thus the development process can be accelerated. Of course, the simulation results must be validated in final tests on textiles.

(e) A bionic floating oil adsorber and collector

The basic concept for a bionic oil adsorber (BOA) is shown in figure 9. The device consists of a buoyant container with the oil-adsorbing textile attached at the edge. One textile end protrudes into the oil-collecting container and is permanently under the water surface/oil film level. The other end protrudes into the contaminated water (e.g. lake). This submerged portion initially holds an air film, which subsequently is substituted by oil adsorbed and transported to the storage container. The transport is maintained until all oil is collected or the oil level in the container is at equal height to the water surface/oil film level outside of the container. In this case, the transport stops. The full container can easily be emptied and the device could be re-used. Based on our data, we estimate that with a BOA having an oil contact line with a length of 1 m, for example, about 1 kg of oil could be removed from a lake surface per hour.

4. Conclusion

The novel passive BOA for the removal of oil films from water surfaces offers a wide range of applications.

The capacity for oil uptake and transport is mainly dependent on three factors: viscosity of the oil, distance of the microstructures on the surface and their wetting behaviour.

The oil uptake capacity strongly depends on the surface structures and the viscosity of the oil. Dense structures are advantageous, but the length of the structures also plays a role since, depending on the viscosity of the oil, oil layers of different thicknesses can be captured on the surfaces. In terms of the transport speed, oils with a low viscosity in combination with dense surface structures allow a faster transport.

An oil transport speed of up to $10\,\mathrm{g\,h^{-1}}$ was measured over a cross-section of $1\,\mathrm{cm^2}$, which is maintained over the eight weeks duration of the experiment. An increase in the length of the contact line between the oil and the bionic adsorbent to 1 m would thus result in 1 kg of oil being adsorbed and transported per hour. This is comparable to the 'accidental everyday pollution'. These results are consistent with the simulations undertaken in this study.

Our results build the basis for the development of a prototypical bionic oil-adsorbing textile and for the construction of a floating oil collector which can be used as a passive device for oil spill clean-up and water purification.

Data accessibility. Videos showing the oil uptake on three superhydrophobic surfaces (*S. molesta*, flock and *P. stratiotes*) are provided in the electronic supplementary material.

Authors' contributions. W.B. had the basic idea for the research project and experimental set-ups. He coordinated our working group. He selected and interpreted the biological role models for the project. M.Mo. did the first experiments on biological and technical surfaces and designed, developed and built the prototype of the floating oil adsorber. I.N. selected and characterized the technical material for the investigations and evaluated the results. M.A. and J.W. are working on the simulative description of the oil transport. In detail, a simplified 3D surface structure model has been developed which describes the oil transport and the phase interaction. This was implemented with computational fluid dynamics simulations of the volume of fluid (VoF) method in ANSYS Fluent. Based on the models, the design parameters are determined in advance and validated in further experiments. N.R. together with M.Ma. did the experiments on technical surfaces (vertical oil transport, adsorption capacities, long-term experiments, etc.). L.K.-T. together with M.Ma. did the

experiments on biological surfaces (vertical oil transport, adsorption capacities, etc.). M.A.K.A. recorded the oil adsorption videos of *Pistia* and flock surfaces. K.K. did the experiments to analyse transport and adsorption on conventional yarns and textiles. T.G. coordinated the work in our working group and together with I.N. selected and evaluated the technical materials. M.Ma. did the experiments on technical and biological surfaces together with L.K.-T. and N.R., and coordinated the work for the writing of the manuscript.

Competing interests. We declare we have no competing interests.

Funding. The research was funded by the Deutsche Bundesstiftung Umwelt (DBU) in the project 'Bionic Oil Adsorber (BOA)—Entwicklung eines physikalischen bionischen Verfahrens zur Entfernung von Ölverschmutzungen auf Wasser unter Einsatz superhydrophober Funktionstextilien'. Project no. 34602/01-23.

Acknowledgements. We acknowledge our colleagues and students. Various companies mentioned in the materials and method section have provided material for the study. We thank the Karlsruhe Nano Micro Facility (KNMF, https://www.kit.edu/knmf) at Karlsruhe Institute of Technology (KIT) for support. The Technology Transfer Department of the University of Bonn and the PROvendis agency were most helpful in transfer and patenting procedures. We thank Dr Amool Raina and Jeanette Ortega, ITA Aachen, for critically revising the English text.

References

1. Fingas MF (ed.). 2015 *Handbook of oil spill science and technology*. Hoboken, NJ: John Wiley. (doi:10.1002/9781118989982)
2. Barthlott W, Rafiqpoor MD, Erdelen WR. 2016 Bionics and biodiversity—bio-inspired technical innovation for a sustainable future. In *Biomimetic research for architecture and building construction—biological design and integrative structures* (eds J Knippers, KG Nickel, T Speck), pp. 11–55. Cham, Switzerland: Springer International. (doi:10.1007/978-3-319-46374-2_3)
3. Atlas RM, Hazen TC. 2011 Oil biodegradation and bioremediation: a tale of the two worst spills in US history. *Environ. Sci. Technol.* **45**, 6709–6715. (doi:10.1021/es2013227)
4. Fingas M. 2012 *The basics of oil spill cleanup*. Boca Raton, FL: CRC Press. (doi:10.1201/b13686)
5. Etkin DS. 2009 *Analysis of U.S. Oil Spillage*. API Publication 356. Washington, DC: American Petroleum Institute.
6. Weis JS. 2014 *Marine pollution: what everyone needs to know*, 1st edn. Oxford, UK: Oxford University Press.
7. Walker A. 2017 Chapter 1—Oil spills and risk perceptions. In *Oil spill science and technology*, 2nd edn (ed. M Fingas), pp. 1–70. Cambridge, MA: Gulf Professional Publishing. (doi:10.1016/B978-0-12-809413-6.00001-1)
8. Davidson WF, Lee K, Cogswell A. 2008 *Oil spill response: a global perspective*. Berlin, Germany: Springer. (doi:10.1007/978-1-4020-8565-9)
9. Helle I, Jolma A, Venesjärvi R. 2016 Species and habitats in danger: estimating the relative risk posed by oil spills in the northern Baltic Sea. *Ecosphere* **7**, e01344. (doi:10.1002/ecs2.1344)
10. Green J, Trett M (eds). 1989 *The fate and effects of oil in freshwater*. Barking, UK: Elsevier Science. (doi:10.1007/978-94-009-1109-3)
11. Bhushan B. 2019 Bioinspired oil–water separation approaches for oil spill clean-up and water purification. *Phil. Trans. R. Soc. A* **377**, 20190120. (doi:10.1098/rsta.2019.0120)
12. Nordvik AB, Simmons JL, Bitting KR, Lewis A, Strøm-Kristiansen T. 1996 Oil and water separation in marine oil spill clean-up operations. *Spill Sci. Technol. Bull.* **3**, 107–122. (doi:10.1016/S1353-2561(96)00021-7)
13. Deng D, Prendergast DP, MacFarlane J, Bagatin R, Stellacci F, Gschwend PM. 2013 Hydrophobic meshes for oil spill recovery devices. *ACS Appl. Mater. Interfaces.* **5**, 774–781. (doi:10.1021/am302338x)
14. Dave D, Ghaly AE. 2011 Remediation technologies for marine oil spills: a critical review and comparative analysis. *Am. J. Environ. Sci.* **7**, 423. (doi:10.3844/ajessp.2011.423.440)
15. Wang S, Li M, Lu Q. 2010 Filter paper with selective absorption and separation of liquids that differ in surface tension. *ACS Appl. Mater. Interfaces.* **2**, 677–683. (doi:10.1021/am900704u)
16. Zeiger C, Kumberg J, Vüllers F, Worgull M, Hölscher H, Kavalenka MN. 2017 Selective filtration of oil/water mixtures with bioinspired porous membranes. *RSC Adv.* **7**, 32 806–32 811. (doi:10.1039/C7RA05385A)

17. Baig N, Alghunaimi FI, Saleh TA. 2019 Hydrophobic and oleophilic carbon nanofiber impregnated styrofoam for oil and water separation: a green technology. *Chem. Eng. J.* **360**, 1613–1622. (doi:10.1016/j.cej.2018.10.042)
18. Barthlott W, Mail M, Neinhuis C. 2016 Superhydrophobic hierarchically structured surfaces in biology: evolution, structural principles and biomimetic applications. *Phil. Trans. R. Soc. A* **374**, 20160191. (doi:10.1098/rsta.2016.0191)
19. Barthlott W, Mail M, Bhushan B, Koch K. 2017 Plant surfaces: structures and functions for biomimetic innovations. *Nano-Micro Lett.* **9**, art. no. 23. (doi:10.1007/s40820-016-0125-1)
20. Barthlott W, Mail M, Bhushan B, Koch K. 2017 Plant surfaces: structures and functions for biomimetic applications. In *Springer handbook of nanotechnology* (ed. B Bhushan), pp. 1265–1305. Berlin, Germany: Springer. (doi:10.1007/978-3-662-54357-3_36)
21. Barthlott W, Neinhuis C. 1997 Purity of the sacred lotus. *Planta* **202**, 1–8. (doi:10.1007/s004250050096)
22. Barthlott W *et al.* 2010 The *Salvinia* paradox: superhydrophobic surfaces with hydrophilic pins for air retention under water. *Adv. Mater.* **22**, 2325–2328. (doi:10.1002/adma.200904411)
23. Mayser MJ, Bohn HF, Reker M, Barthlott W. 2014 Measuring air layer volumes retained by submerged floating-ferns *Salvinia* and biomimetic superhydrophobic surfaces. *Beilstein J. Nanotechnol.* **5**, 812–821. (doi:10.3762/bjnano.5.93)
24. Amabili M, Giacomello A, Meloni S, Casciola CM. 2015 Unraveling the *Salvinia* paradox: design principles for submerged superhydrophobicity. *Adv. Mater. Interfaces* **2**, 1500248. (doi:10.1002/admi.201500248)
25. Marmur A. 2006 Super-hydrophobicity fundamentals: implications to biofouling prevention. *Biofouling* **22**, 107–115. (doi:10.1080/08927010600562328)
26. Mail M *et al.* 2018 A new bioinspired method for pressure and flow sensing based on the underwater air-retaining surface of the backswimmer *Notonecta*. *Beilstein J. Nanotechnol.* **9**, 3039–3047. (doi:10.3762/bjnano.9.282)
27. Gorb EV, Hofmann P, Filippov AE, Gorb SN. 2017 Oil adsorption ability of three-dimensional epicuticular wax coverages in plants. *Sci. Rep.* **7**, 45483. (doi:10.1038/srep45483)
28. Zeiger C, Rodrigues da Silva IC, Mail M, Kavalenka MN, Barthlott W, Holscher H. 2016 Microstructures of superhydrophobic plant leaves—inspiration for efficient oil spill cleanup materials. *Bioinspir. Biomim.* **11**, 056003. (doi:10.1088/1748-3190/11/5/056003)
29. Bhushan B. 2018 Lessons from nature for green science and technology: an overview and bioinspired superliquiphobic/philic surfaces. *Phil. Trans. R. Soc. A* **377**, 20180274. (doi:10.1098/rsta.2018.0274)
30. Koch K, Barthlott W. 2009 Superhydrophobic and superhydrophilic plant surfaces: an inspiration for biomimetic materials. *Phil. Trans. R. Soc. A* **367**, 1487–1509. (doi:10.1098/rsta.2009.0022)
31. Wistuba N. 2000 Untersuchungen zum Mechanismus des Wassertransportes in höheren Pflanzen mit Hilfe der Druckmesssonden- und NMR-Bildgebungstechnik. PhD thesis, University of Würzburg, Germany.
32. Bashir S, Rees JM, Zimmerman WB. 2011 Simulations of microfluidic droplet formation using the two-phase level set method. *Chem. Eng. Sci.* **66**, 4733–4741. (doi:10.1016/j.ces.2011.06.034)
33. Chen C, Zhao Y, Wang J, Zhu P, Tian Y, Xu M, Wang L, Huang X. 2018 Passive mixing inside microdroplets. *Micromachines* **9**, 160. (doi:10.3390/mi9040160)
34. ANSYS. 2017 *ANSYS Fluent tutorial guide*, Release 18. ANSYS, Inc., Canonsburg, PA.
35. Hollebone B. 2017 Chapter 3—Oil physical properties: measurement and correlation. In *Oil spill science and technology*, 2nd edn (ed. M Fingas), pp. 185–207. Cambridge, MA: Gulf Professional Publishing. (doi:10.1016/B978-0-12-809413-6.00003-5)
36. Barthlott W, Wiersch S, Čolić Z, Koch K. 2009 Classification of trichome types within species of the water fern *Salvinia*, and ontogeny of the egg-beater trichomes. *Botany* **87**, 830–836. (doi:10.1139/B09-048)
37. Huang W, Bhullar RS, Fung YC. 2001 The surface-tension-driven flow of blood from a droplet into a capillary tube. *J. Biomech. Eng.* **123**, 446–454. (doi:10.1115/1.1389096)